Available online at www.sciencedirect.com
ScienceDirect
Journal of the European Ceramic Society 28 (2008) 229–233
www.elsevier.com/locate/jeurceramsoc

Microstructure and material properties of double-network type fibrous (Al_2O_3–m-ZrO_2)/t-ZrO_2 composites

Byong-Taek Lee [a,*], Swapan Kumar Sarkar [b], Ho-Yeon Song [c]

[a] *Department of Biomedical Engineering and Materials, School of Medicine, Soonchunhyang University 366-1, Ssangyoung-dong, Cheonan, Chungnam 330-090, South Korea*
[b] *School of Advanced Materials Engineering, Kongju National University, 182, Shinkwan-dong, Kongju, Chungnam 314-701, South Korea*
[c] *Department of Microbiology, School of Medicine, Soonchunhyang University 366-1, Ssangyoung-dong, Cheonan, Chungnam 330-090, South Korea*

Received 20 February 2007; received in revised form 7 May 2007; accepted 13 May 2007
Available online 2 August 2007

Abstract

Al_2O_3–(m-ZrO_2)/t-ZrO_2 composites with a novel double-network microstructure were fabricated by multi-pass extrusion process using polymer bound ceramic green body. A simultaneous micro- and macro-level microstructure tailoring was made where unidirectionally aligned two-phase Al_2O_3–(m-ZrO_2) fibers were enclosed in a t-ZrO_2 phase connected in a network formation and this network was further enclosed in a thicker t-ZrO_2 phase. Composite green rods were hot extruded and reassembled in parallel for extrusion and after several passes of extrusion very fine microstructure with dimension of a few micrometers was obtained. Material properties such as hardness, bending strength and fracture toughness were measured for the composites. Microstructure characterization was carried out by SEM technique. In the 4th passed Al_2O_3–(m-ZrO_2)/t-ZrO_2 composites, the outer network of t-ZrO_2 was 15 μm, inner network 0.8 μm and the inner Al_2O_3–(m-ZrO_2) core was 2.5 μm. The highest hardness, fracture strength and toughness values were about 1452 Hv, 1006 MPa and 8.6 MPa $m^{1/2}$, respectively, in the sample sintered at 1500 °C.

Keywords: Extrusion; Composites; Microstructure-final; Al_2O_3; ZrO_2

1. Introduction

Alumina (Al_2O_3) is one of the high performance ceramics used in high-temperature, structural, cutting and wear resistance applications.[1,2] The excellent chemical stability and bio-inertness extends its application for harsh environment and biomedical applications.[3,4] However, there is a common drawback of Al_2O_3 like most other ceramics, i.e., it has poor fracture toughness (about 3.5 MPa $m^{1/2}$), which is a hindrance for use in dynamic load-bearing applications.[5] This is basically due to the absence of main toughening mechanisms such as microcracks, crack bridging, phase transformation, etc. Hence, many strategies have been proposed to improve the mechanical properties of a monolithic Al_2O_3 body. Dispersion of ZrO_2 in the Al_2O_3 matrix has been found to be effective for fracture toughening due to phase transformation from tetragonal (t) to monoclinic (m). In case of the dispersion of m-ZrO_2 particles in the Al_2O_3 matrix, the strong strain field and some microcracks were easily formed during the sintering process, due to the difference in the co-efficient of thermal expansion.[6] These strain fields and microcracks led to intergranular fracture with crack deflection and thus reduce the crack propagation energy.[3] In addition when cracks propagate transgranularly in m-ZrO_2 the driving force of crack propagation is reduced due to the plastic deformation of m-ZrO_2.[6,7] In conjunction to this many other approaches have also been investigated for the improvement of fracture toughness like metal coating of raw ceramic powder for metal–ceramic composites, whisker and particle reinforcements.[8,9] Incorporation of metal as a fracture toughening agent hinders high temperature applications, and dealing with whiskers poses the possibility of health hazards.[10] Microstructural modification of the composites systems is a way for improving the fracture toughness. The multi-pass extrusion method has a remarkable potential in this regard, because

* Corresponding author. Tel.: +82 41 570 2427; fax: +82 41 577 2415.
E-mail address: lbt@sch.ac.kr (B.-T. Lee).

0955-2219/$ – see front matter © 2007 Elsevier Ltd. All rights reserved.
doi:10.1016/j.jeurceramsoc.2007.05.010

the microstructure can be tailored with many desired features like fibrous microstructure,[11] fibrous microstructure with soft interface,[12] etc., which can impart some unique characteristics. In the fibrous monolithic process, the ceramic powder is mixed with polymer to make an extrudable material and extrusion is carried out. Selecting combination of materials and changing the arrangements of filaments during loading for extrusion, various kinds of microstructures can be fabricated. In our previous work, we fabricated continuously porous Al_2O_3,[4] ZrO_2[13] and their composites.[2,14] A coating of HAp inside the continuous pores of ZrO_2[15] and functionally gradient HAp–(t-ZrO_2)/Al_2O_3–(m-ZrO_2) composites[16] were fabricated by the same method.

In this work, as a new approach, to improve the fracture strength and toughness, a novel double-network type microstructure with fibrous (Al_2O_3–m-ZrO_2)/t-ZrO_2 composites were fabricated using the multi-pass extrusion process. To utilize the phase transformation toughening mechanism of t-ZrO_2, a network boundary was fabricated surrounding the fine core/shell microstructure of (Al_2O_3–m-ZrO_2)/t-ZrO_2 where the adjoining t-ZrO_2 shell phase forms a continuous inner network. In the two-phase core 25 vol.% m-ZrO_2 was dispersed in Al_2O_3 matrix. This was done decrease the grain coarsening and to introduce microcracking near the phase boundary of Al_2O_3 and m-ZrO_2, which is reported to improve the fracture toughness of the system as stated earlier. A thicker outer cylinder of t-ZrO_2 enclosed this assembly and all the cylinders made a formation of macro-scale network. The microstructure of the fabricated material contained sub-micrometer level dimension which renders the use of nanopowders obvious. It also improves the mechanically property of the composite compared to the coarse powder. In the work the microstructural details were characterized with the SEM technique. Hardness, relative density, bending strength and fracture toughness was investigated for different sintering temperatures.

2. Experimental procedure

Alumina (α-Al_2O_3, about 300 nm, AKP-50, Sumitomo, Japan), monoclinic zirconia (m-ZrO_2, about 80 nm, Tosoh Corporation, Nanyo Manufacturing Complex, Japan), tetragonal zirconia (t-ZrO_2, about 80 nm, Tosoh Corporation, Nanyo Manufacturing Complex), ethylene vinyl acetate (EVA) (ELVAX 210 and 250, Dupont, USA) and stearic acid ($CH_3(CH_2)_{16}COOH$, Daejung Chemicals & Metals Co., Korea) were used as starting materials. 75 vol.% Al_2O_3 and 25 vol.% m-ZrO_2 powders were homogeneously mixed in ethanol by ball milling using Al_2O_3 balls. (Al_2O_3/m-ZrO_2)/EVA/stearic acid (volume ratio, 50:40:10) and t-ZrO_2/EVA/stearic acid (volume ratio, 47:40:13) were separately mixed using a shear mixture (C.W. Brabender Instruments, Shina Platech Co., Hwaseong Gyeong-Gi-Do, Korea). The polymer bound (Al_2O_3/m-ZrO_2) and t-ZrO_2 mixtures were used to make rod-like cores (22 mm diameter) and tube-like shells (4 mm thick) by warm press, respectively. This t-ZrO_2 shell makes the inner network of the final composites. These core and shell were assembled together to prepare the feed roll which consisted of 60/40 volume fraction of the core and shell. The feed roll was then extruded at 120 °C with 8 mm/min extrusion velocity to make the 1st passed filaments, which were 3.5 mm in diameter. The 1st passed filaments were cut 80 mm length and reloaded in a steel die and again rod-like cores were prepared (22 mm diameter). Then, these core and previously prepared t-ZrO_2 shell were assembled again and extruded to make the 2nd passed filaments, 3.5 mm in diameter. The t-ZrO_2 shell in this stage will make the outer network of the final composites. The 2nd passed filaments were cut and reloaded to make the 3rd passed filaments. Subsequently, the 4th passed filaments were made in the same way by assembling and extruding the 3rd passed filaments. To obtain the sintered body from these green composites, first a binder burning-out process was carried out at 700 °C for 2 h in a N_2 atmosphere with a very slow heating rate and then again at 1000 °C for 2 h in an air atmosphere. Finally, the pressureless sintering process was carried out at different temperatures ranging from 1300 to 1500 °C for 1 h in an air atmosphere.

Microstructures and fracture surfaces were observed using a scanning electron microscope (SEM, JSM-6335F, JEOL, Japan). The relative density was measured by the Archimedes method. The average bending strength was measured by a four-point bending test method with a universal testing machine (Unitech TM, R&B, Korea) using eight specimens (2.75 mm in diameter × 30 mm in length) with a crosshead speed of 0.1 mm/min. To measure the Vickers hardness and fracture toughness, 2.75 mm diameter cylindrical-shaped samples were cut about 4 mm in length and polished, using up to 1 μm diamond paste. The average Vickers hardness was measured by indenting with a load of 5 kg (10 points/sample). The fracture toughness was calculated by the indentation method using an indentation load of 10 kg.

3. Results and discussion

Fig. 1 shows the cross-sectional SEM micrographs of the double-network type fibrous (Al_2O_3–m-ZrO_2)/t-ZrO_2

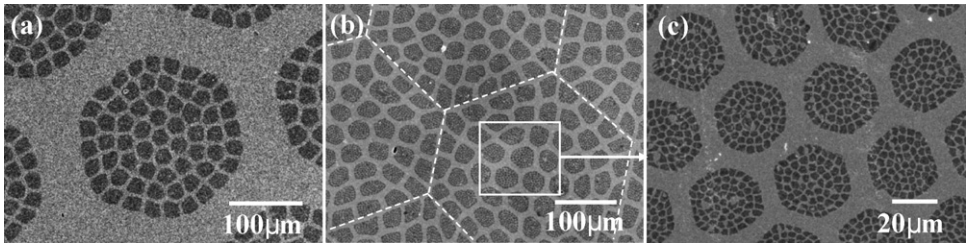

Fig. 1. SEM micrographs of (a) 3rd and (b and c) 4th passed double-network type fibrous Al_2O_3–(m-ZrO_2)/t-ZrO_2 composite sintered at 1500 °C.

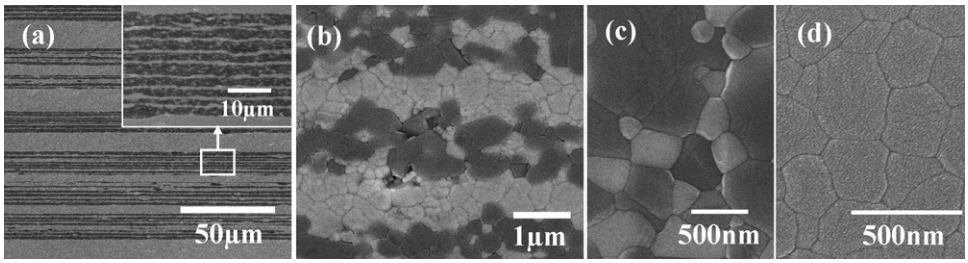

Fig. 2. Longitudinal SEM micrographs of (a and b) 4th passed double-network type fibrous Al_2O_3–(m-ZrO_2)/t-ZrO_2 composite and enlarged SEM image from (c) Al_2O_3–(m-ZrO_2) core and (d) t-ZrO_2 outer network regions.

composites sintered at 1500 °C. Fig. 1(a) was taken from the 3rd passed filament and shows the unit microstructure of the tailored composites. The dark contrasts in the image which were the two-phase (Al_2O_3–m-ZrO_2) cores were encircled by t-ZrO_2 cylinder, observed as white contrast in the SEM image. The t-ZrO_2 enclosures of the cores were adjoined in an interconnected formation and made a network-like microstructural arrangement. This entire arrangement is confined within the boundary of another t-ZrO_2 enclosure, evident in the SEM image by the thicker white contrast. This outer t-ZrO_2 phase is adjoined with the bordering of the same kind and made a network type formation. This outer network of t-ZrO_2 is more clearly evident in the 4th passed SEM image in Fig. 1(b). The microstructure has just been scaled down in dimension in the 4th passed filament from the 3rd passed filament keeping its design the same. Ultimately it was observed that a t-ZrO_2 network was enclosing a two-phase system of Al_2O_3–(m-ZrO_2) which itself was enclosed within a networked t-ZrO_2 phase. This type of a network-like microstructure inside another network led to think this microstructure as a double-network type microstructure and this group of words was used through the manuscript to describe this hierarchically oriented microstructure. In Fig. 1(c), the enlarged SEM image of the 4th passed filament showed clearly the double network of the t-ZrO_2 phase.

The thicknesses of the outer and inner t-ZrO_2 network in the 3rd passed composite were about 60 and 3 μm, respectively, and the Al_2O_3–(m-ZrO_2) core was about 25 μm in diameter. In the 4th passed composite the Al_2O_3–(m-ZrO_2) core was about 2.5 μm in diameter and the outer and inner t-ZrO_2 shell thicknesses were about 15 and 0.8 μm, respectively. The outer network appeared almost hexagonal in shape. This shape is attributed to the arrangement of the 1st passed filaments in the die which follow a near hexagonal assembly. The inner micro-groups also exhibit the same geometric feature. The hexagonal shape is also retained in the 4th passed composites as shown in Fig. 1(c). Moreover, the hexagonal cells containing the typical double-network microstructures were seen as indicated by the dotted lines in Fig. 1(b). These were the individual 3rd passed filaments. However, as the number of extrusion passes increased, the microstructure became finer and ultimately the inner network thickness became sub-micrometer as shown in Fig. 1(c). This is a unique way to fabricate a hierarchically arranged microstructure where the lowest microstructural dimension can reach even up to sub-micrometer level. The microstructure did not show any bulk defects such as cracks and delamination between Al_2O_3–(m-ZrO_2) cores and t-ZrO_2 shells during the sintering process. Using one pass further, a modified nanostructured composite can be made by this top down fabrication process. However, using the present technology it can be easily conceived that, N extrusion passes might be expected to lead to an $(N-2)$ network type microstructure, provided that the particle size of the constituent materials are significantly lower compared to the lowest dimension achievable for the inner network thickness.

Fig. 2 shows the longitudinal SEM micrographs of (a) 4th passed double-network type composites sintered at 1500 °C. A homogeneous, fibrous microstructure with a highly unidirectional orientation was observed in the low magnification image (a). From this image the hierarchical sub-micrometer and micro-level orientation of t-ZrO_2 phase was confirmed. The Al_2O_3–(m-ZrO_2) core was also observed in unidirectional alignment where the thickness was about 2.5 μm. The inserted image in Fig. 2(a) clearly depicted this point. In the thermal etched enlarged image (b), the t-ZrO_2 shells and Al_2O_3–(m-ZrO_2) cores comprised a dense microstructure without any deleterious phenomena like cracking, delimitation, etc. This result indicated that the submicron-sized continuous fibrous microstructures were well controlled using the multi-pass extrusion process. Enlarged SEM images (c and d) were taken from the Al_2O_3–(m-ZrO_2) core and t-ZrO_2 shell regions, respectively. In the enlarged image of Al_2O_3–(m-ZrO_2) core (c), the bright and dark contrasts were m-ZrO_2 and Al_2O_3 phases, respectively. The average Al_2O_3 grain size was about 0.7 μm in diameter while the m-ZrO_2 grain was about 0.3 μm in diameter. However, most of the fine m-ZrO_2 phases were located in the Al_2O_3 grain boundary. The presence of m-ZrO_2 phase in the core region decreased the grain growth of Al_2O_3, which undergoes excessive grain coarsening during high temperature sintering. The average grain size of the t-ZrO_2 outer network was about 0.4 μm in diameter as shown in Fig. 2(d). Although the particle size of m-ZrO_2 and t-ZrO_2 was same initially, after sintering the grain size was different due to the pinning effect. In the Al_2O_3–(m-ZrO_2) core the m-ZrO_2 was surrounded by Al_2O_3 grains and grain growth was hindered.

Fig. 3 shows the relative density and bending strength of 4th passed double-network type fibrous (Al_2O_3–m-ZrO_2)/t-ZrO_2 composites depending on the sintering temperature. The bending test was performed on the round bar with smooth surface without any additional surface preparation. The following equation was used to calculate the bending strength of the samples

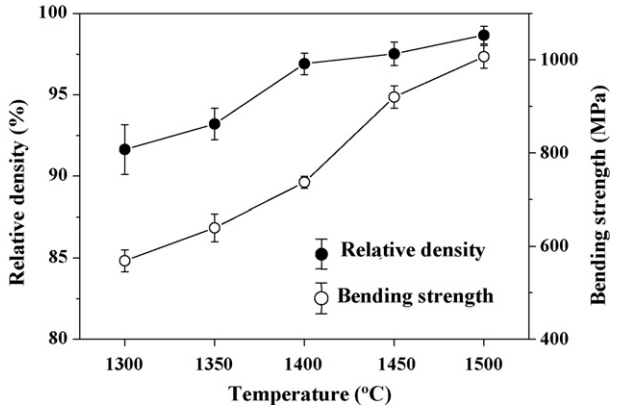

Fig. 3. Relative density and bending strength of 4th passed network type fibrous Al_2O_3–(m-ZrO_2)/t-ZrO_2 composites.

where the span length for the testing apparatus was 10 mm.

$$\text{Bending strength} = 16l\frac{m}{\pi}D^3\left(\frac{1}{0.1013}\right)$$

where l is the load (kg), m the span length (mm) and D is the diameter of the bend bar (mm).

In the sample sintered at 1300 °C, the values of the relative density and bending strength were comparatively low with about 91% and 567 MPa, respectively, due to low densification. However, as the sintering temperature increased, the values increased due to the enhanced densification. The maximum relative density and bending strength values were obtained at 1500 °C and their values were about 98.5 and 1006 MPa, respectively. These values are higher than those of individual monolithic ceramics.[17] Compared to the other network type (Al_2O_3–m-ZrO_2)/t-ZrO_2 composites,[11] the value of the bending strength also increased. The fibrous, hierarchical microstructure imparted this superior mechanical property.

Fig. 4 shows the hardness and fracture toughness of 4th passed network type fibrous (Al_2O_3–m-ZrO_2)/t-ZrO_2 composites depending on the sintering temperature. The fracture toughness was measured in both longitudinal and transverse sections of the composites. As the sintering temperature increased,

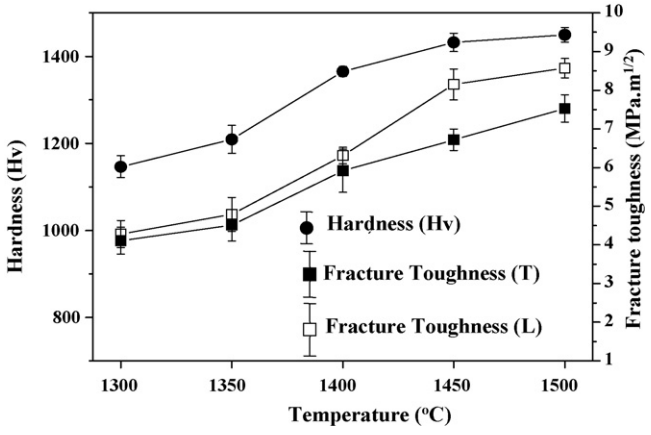

Fig. 4. Hardness and fracture toughness of 4th passed network type fibrous Al_2O_3–(m-ZrO_2)/(t-ZrO_2) composites depending on sintering temperature.

the values of hardness and fracture toughness increased gradually due to the increased densification of the composite. The hardness values of the 4th passed network type fibrous (Al_2O_3–m-ZrO_2)/t-ZrO_2 composites sintered at 1300 and 1500 °C were about 1149 and 1452 Hv, respectively. To investigate the trend of the fracture toughness, K_{IC} was measured by the indentation method using Evan's equation. The equation is,

$$K_{IC} = 0.16Ha^{1/2}\left(\frac{c}{a}\right)^{-3/2}$$

where H is the Vickers hardness, a the half of indentation diagonal and c is the half of crack length from indentation center.

In the sample sintered at 1300 °C the values of fracture toughness in both the longitudinal and transverse sections were comparatively low, about 4.8 and 4.7 MPa $m^{1/2}$, respectively. However, their values increased with the sintering temperature and at 1500 °C the maximum fracture toughness in the longitudinal and transverse sections were about 8.6 and 7.4 MPa $m^{1/2}$, respectively. However, in the transverse section, the fracture toughness values were slightly lower than those in the longitudinal section due to the orientation of the fibrous microstructure. In the transverse section the crack tip traveled along axis which was almost symmetrical in morphology. The crack tip had to cross the inner core/sell arrangement (Al_2O_3–m-ZrO_2)/t-ZrO_2 and the outer thick boundary of t-ZrO_2. The crack propagation energy was dissipated by the microcracks of the two-phase core and by the t–m phase transformation of the t-ZrO_2 phases of the inner and outer network. However, in case of the indentation in the longitudinal section the crack tip had to travel across the unidirectionally aligned inner and outer t-ZrO_2 cylinders and the (Al_2O_3–m-ZrO_2) fibers. The unidirectional orientation of the phases imparts slightly higher fracture toughness. In case of the crack propagation along the axis of the fibrous alignment the cylindrical confinement by the inner and outer network of t-ZrO_2 hinders the crack tip to propagate along the weaker (Al_2O_3–m-ZrO_2) core phase and the crack length was comparable in the two anisotropic axes in the longitudinal section.

Fig. 5 shows the SEM fracture surfaces of the 4th passed network type (Al_2O_3–m-ZrO_2)/t-ZrO_2 composites sintered at 1500 °C. In Fig. 5(a), the fracture surface shows the outer t-ZrO_2 network and inner (Al_2O_3–m-ZrO_2)/t-ZrO_2 network. However, in the inner (Al_2O_3–m-ZrO_2)/t-ZrO_2 zone, a rougher surface is observed compared to the outer t-ZrO_2 network zone, which was due to the effect of the fibrous microstructure. This phenomenon indicates that the microstructure had an effect on the fracture propagation path. The higher roughness means higher deflection of the crack propagation path which in turn can improve the fracture toughness of the composites. In Fig. 5(b and c), the enlarged images of the fracture surface of the outer and inner network are shown. The outer t-ZrO_2 network zone had a mixed fracture mode with both inter- and trans-granular fractures, whereas, in the inner (Al_2O_3–m-ZrO_2)/t-ZrO_2 zone the fracture mode also showed a mixed fracture mode with the Al_2O_3 phase predominantly in the trans-granular mode of fracture. In previous reports the fibrous monolithic ceramic was fabricated by the Si_3N_4/BN system with a soft interface in which strong delamination dur-

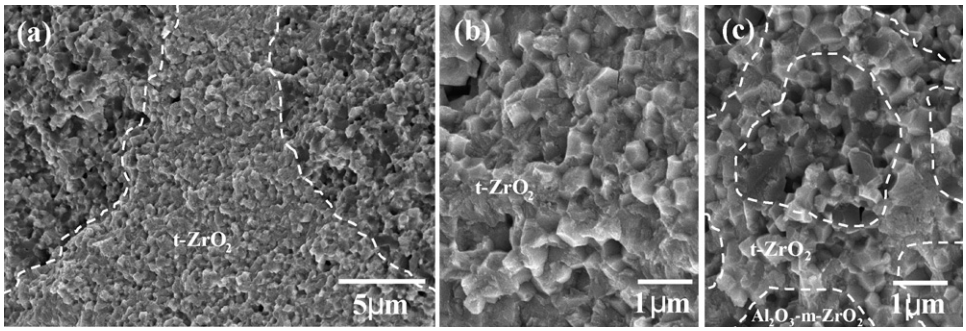

Fig. 5. SEM fracture surfaces of 4th passed network type fibrous Al_2O_3–(m-ZrO_2)/t-ZrO_2 composite sintered at 1500 °C. Low magnification image (a) and enlarged images of outer (b) and inner network (c) of the composites.

ing fracture occurred and fibrous morphology was evident.[12,18] But in our system with the same kind of microstructure the Al_2O_3/ZrO_2 system had a very rigid interface with a strong interfacial bonding. That's why the fracture surface did not show any fibrous pull out or delamination despite having a fibrous morphology.

4. Conclusions

(Al_2O_3–m-ZrO_2)/t-ZrO_2 composites with a double-network type fibrous microstructure were fabricated by the multi-pass extrusion process using polymer mixed ceramic powders in an extrudable state. The relationship between microstructure and material properties depending on the sintering temperature were investigated. Homogeneous and hierarchical microstructures with unidirectional alignment of the single and two-phase system were successfully obtained and their structures became fine as the number of extrusion passes increased. The thicknesses of the t-ZrO_2 phase of the outer and the inner network of the 4th passed samples were about 15 and 0.8 μm, respectively, and that of the (Al_2O_3–m-ZrO_2) core of the inner network was 2.5 μm. On the other hand, as the sintering temperature increased, the material properties such as hardness, bending strength, fracture toughness of the 4th passed network type fibrous (Al_2O_3–m-ZrO_2)/t-ZrO_2 composites increased remarkably. In the samples sintered at 1500 °C, maximum values of about 1452 Hv, 1006 MPa and 8.6 MPa $m^{1/2}$, respectively, were obtained. However, the fracture toughness value in the transverse direction was slightly lower than that in the longitudinal direction due to the fibrous microstructure.

Acknowledgements

This work was supported by the Korea Science and Engineering Foundation (KOSEF) through the 'National Research Lab' program funded by the Ministry of Science and Technology. The authors would like to thank Mr. Asit Kumar Gain for his earnest effort in the experimentation.

References

1. Ravikiran, A., Influence of apparent pressure on wear behavior of self-mated alumina. *J. Am. Ceram. Soc.*, 2002, **83**, 1302.
2. Lee, B. T., Sarkar, S. K., Gain, A. K., Yim, S. J. and Song, H. Y., Core/shell volume effect on the microstructure and mechanical properties of fibrous Al_2O_3–(m-ZrO_2)/t-ZrO_2 composite. *Mater. Sci. Eng. A*, 2006, **432**, 317.
3. Lee, B. T., Nishiyama, A. and Hiraga, K., Micro-indentation fracture behavior of Al_2O_3–24 vol% $ZrO_2(Y_2O_3)$ composites studied by transmission electron microscopy. *Mater. Trans., JIM*, 1993, **34**, 682.
4. Lee, B. T., Kang, I. C., Cho, S. H. and Song, H. Y., Fabrication of a continuously oriented porous Al_2O_3 body and its in vitro study. *J. Am. Ceram. Soc.*, 2005, **88**, 2262.
5. Munro, R. G., Evaluated material properties for a sintered alpha-alumina. *J. Am. Ceram. Soc.*, 1997, **80**, 1919.
6. Lee, B. T., Lee, K. H. and Hiraga, K., Stress-induced phase transformation of ZrO_2 in ZrO_2 (3 mol% Y_2O_3)–25 vol% Al_2O_3 composite studied by transmission electron microscopy. *Scripta Mater.*, 1998, **38**, 1101.
7. Lee, B. T. and Hiraga, K., Crack propagation and deformation behavior of Al_2O_3–24 vol% ZrO_2 composite studied by transmission electron microscopy. *J. Mater. Res.*, 1994, **9**, 1199.
8. Zhan, G. D., Kuntz, J. D., Duan, R. G. and Mukherjee, A. K., Spark-plasma sintering of silicon carbide whiskers (SiC_w) reinforced nanocrystalline alumina. *J. Am. Ceram. Soc.*, 2004, **87**, 2297.
9. Levin, I., Kaplan, W. D., Brandon, D. G. and Layyous, A. A., Effect of SiC submicrometer particle size and content on fracture toughness of alumina–SiC "nanocomposites". *J. Am. Ceram. Soc.*, 1995, **78**, 254.
10. Wang, L., Jiang, W. and Chen, L., Fabrication and characterization of nano-SiC particles reinforced TiC/SiC_{nano} composites. *Mater. Lett.*, 2004, **58**, 1401.
11. Lee, B. T., Kim, K. H. and Han, J. K., Microstructure and material properties of fibrous Al_2O_3–(m-ZrO_2)/t-ZrO_2 composites fabricated by a fibrous monolithic process. *J. Mater. Res.*, 2004, **19**, 3234.
12. Kovar, D., King, B. H., Trice, R. W. and Halloran, J. W., Fibrous monolithic ceramics. *J. Am. Ceram. Soc.*, 1997, **80**(10), 2471.
13. Gain, A. K. and Lee, B. T., Microstructure control of continuously porous t-ZrO_2 bodies fabricated by multi-pass extrusion process. *Mater. Sci. Eng. A*, 2006, **419**(1–2), 269.
14. Lee, B. T., Jang, D. H., Kang, I. C. and Lee, C. W., Relationship between microstructures and material properties of novel fibrous Al_2O_3–(m-ZrO_2)/t-ZrO_2 composites. *J. Am. Ceram. Soc.*, 2005, **88**, 2874.
15. Gain, A. K. and Lee, B. T., Fabrication of HAp coated micro-channelled t-ZrO_2 bodies by the multi-pass extrusion process. *J. Am. Ceram. Soc.*, 2006, **89**(6), 2051.
16. Lee, C. W., Gain, A. K., Yim, S. J. and Lee, B. T., Microstructure characterization of fibrous HAp–(20 vol.% t-ZrO_2)/Al_2O_3–(25 vol.% m-ZrO_2) composites by multi-pass extrusion process. *Mater. Lett.*, 2007, **61**, 405.
17. Miyazaki, H., Yoshizawa, Y. and Hirao, K., Effect of the volume ratio of zirconia and alumina on the mechanical properties of fibrous zirconia/alumina bi-phase composites prepared by co-extrusion. *J. Eur. Ceram. Soc.*, 2006, **26**, 3539.
18. Trice, R. W. and Halloran, J. W., Influence of microstructure on the interfacial fracture energy of silicon nitride/boron nitride fibrous monolithic ceramics. *J. Am. Ceram. Soc.*, 1999, **82**(9), 2502.